European Radiology (2023) 33:3286–3294
https://doi.org/10.1007/s00330-022-09331-z

MAGNETIC RESONANCE

Capability of arterial spin labeling and intravoxel incoherent motion diffusion-weighted imaging to detect early kidney injury in chronic kidney disease

Wei Mao[1] · Yuqin Ding[1] · Xiaoqiang Ding[2] · Caixia Fu[3] · Bohong Cao[1] · Bernd Kuehn[4] · Thomas Benkert[4] · Robert Grimm[4] · Jianjun Zhou[1,5] · Mengsu Zeng[1]

Received: 2 August 2022 / Revised: 1 November 2022 / Accepted: 28 November 2022 / Published online: 13 December 2022

Abstract

Objectives To prospectively investigate the capability of arterial spin labeling (ASL) and intravoxel incoherent motion diffusion-weighted imaging (IVIM-DWI) for the identification of early kidney injury in chronic kidney disease (CKD) patients with normal estimated glomerular filtration rate (eGFR).

Methods Fifty-four CKD patients confirmed by renal biopsy (normal eGFR group [eGFR ≥ 90 mL/min/1.73 m^2]: n = 26; abnormal eGFR group [eGFR < 90 mL/min/1.73 m^2]: n = 28) and 20 healthy volunteers (HV) were recruited. All subjects were examined by IVIM-DWI and ASL imaging. Renal blood flow (RBF) derived from ASL, true diffusion coefficient (D), pseudo-diffusion coefficient (D*), and perfusion fraction (f) derived from IVIM-DWI were measured from the renal cortex. One-way analysis of variance was used to compare MRI parameters among the three groups. The correlation between eGFR and MRI parameters was evaluated by Spearman correlation analysis. Diagnostic performances of MRI parameters for detecting kidney injury were assessed by receiver operating characteristic (ROC) curves.

Results The renal cortical D, D*, f, and RBF values showed statistically significant differences among the three groups. eGFR was positively correlated with MRI parameters (D: r = 0.299, D*: r = 0.569, f: r = 0.733, RBF: r = 0.586). The areas under the curve (AUCs) for discriminating CKD patients from HV were 0.725, 0.752, 0.947, and 0.884 by D, D*, f, and RBF, respectively. D, D*, f, RBF, and eGFR identified CKD patients with normal eGFR with AUCs of 0.735, 0.612, 0.917, 0.827, and 0.733, respectively, and AUC of f value was significantly larger than that of eGFR.

Conclusion IVIM-DWI and ASL were useful for detecting underlying pathologic injury in early CKD patients with normal eGFR.

Key Points

- *The renal cortical f and RBF values in the control group were significantly higher than those in the normal eGFR group.*
- *A negative correlation was observed between the renal cortical D, D*, f, and RBF values and SCr and 24 h-UPRO, while eGFR was significantly positively correlated with renal cortical D, D*, f, and RBF values.*
- *The AUC of renal cortical f values was statistically larger than that of eGFR for the discrimination between the CKD with normal eGFR group and the control group.*

Keywords Chronic kidney diseases · Functional magnetic resonance imaging · Renal insufficiency

✉ Jianjun Zhou
zhoujianjunzs@126.com

✉ Mengsu Zeng
fdzsmw@126.com

[1] Department of Radiology, Zhongshan Hospital, Shanghai Institute of Medical Imaging, Fudan University, 180 Fenglin Road, Shanghai 200032, People's Republic of China

[2] Department of Nephrology, Zhongshan Hospital, Fudan University, 180 Fenglin Road, Shanghai 200032, People's Republic of China

[3] MR Applications Development, Siemens Shenzhen Magnetic Resonance Ltd, Shenzhen, People's Republic of China

[4] MR Application Predevelopment, Siemens Healthcare GmbH, Erlangen, Germany

[5] Department of Radiology, Zhongshan Hospital, Xiamen Branch, Fudan University, Xiamen, People's Republic of China

Abbreviations

24 h-UPRO	24-h urinary protein
ASL	Arterial spin labeling
AUC	Area under the curve
CKD	Chronic kidney disease
D	True diffusion coefficient
D*	Pseudo-diffusion coefficient
DWI	Diffusion-weighted imaging
eGFR	Estimated glomerular filtration rate
f	Perfusion fraction
ICC	Intraclass correlation coefficients
IVIM-DWI	Intravoxel incoherent motion diffusion-weighted imaging
MRI	Magnetic resonance imaging
pCASL	Pseudo-continuous arterial spin labeling
RBF	Renal blood flow
ROC	Receiver operating characteristic
ROIs	Regions of interest
SCr	Serum creatinine

Introduction

Chronic kidney disease (CKD) is a public health problem associated with high costs and poor outcomes [1, 2]. Clinical practice shows that early diagnosis and treatment can delay the progression of CKD and improve prognosis. Therefore, early diagnosis and evaluation of CKD is extremely important. However, it is challenging to accurately diagnose early CKD using traditional biochemical indexes, especially in patients with stage-1 CKD, whose estimated glomerular filtration rate (eGFR) is normal. Currently, renal biopsy is required for a definite CKD diagnosis. Nevertheless, renal biopsy exposes patients to the potential risks of perirenal hematomas, infection, bleeding, or even death [3]. Furthermore, renal biopsy is unlikely to be readily repeated clinically.

Early CKD should be diagnosed by repeatable and noninvasive techniques. Accordingly, a great deal of interest has been garnered in using functional magnetic resonance imaging (MRI) to assess renal function, which has good reproducibility and non-invasiveness [4]. Conventional monoexponential diffusion-weighted imaging (DWI) reflects a combination of water diffusion and tissue perfusion [5]. Intravoxel incoherent motion diffusion-weighted imaging (IVIM-DWI), which applies a bi-exponential model to MR signal intensity decay, could assess both tissue capillary perfusion and water diffusion [6].

Theoretically, IVIM-DWI might be more sensitive and accurate in assessing renal microstructures and function. Pathologic changes in renal microstructures can be evaluated by its parameters including true diffusion coefficient (D), pseudo-diffusion coefficient (D*), and perfusion fraction (f) [7–9]. Recently, studies have demonstrated that IVIM-DWI could assess renal function in CKD [10, 11] and renal fibrosis [12–14] and evaluate transplant kidney function [15, 16]. Arterial spin labeling (ASL) imaging uses endogenous water molecules as tracers and has been widely used in MR brain imaging previously. Preliminary study of ASL imaging revealed that renal blood flow evaluated by para-aminohippuric acid plasma clearance corresponded well to ASL [17]. Previous studies have demonstrated that ASL imaging could assess renal perfusion in CKD [18] and evaluate renal pathologic alterations in acute kidney injury [19].

The purpose of this study was to determine whether IVIM-DWI and ASL imaging could serve as the noninvasive techniques for identifying CKD that requires further evaluation with renal biopsy. Furthermore, we are more interested in assessing the diagnostic performance of IVIM-DWI and ASL imaging for detecting early kidney injury in CKD.

Materials and methods

Subjects

This prospective study was approved by the local ethics committee, and informed consent was obtained from all subjects. Between May 2021 and April 2022, 60 consecutive CKD patients who had received a definitive diagnosis by renal biopsy at our hospital were recruited. The exclusion criteria were as follows: (1) presence of renal neoplastic lesions (diameter > 10 mm), (2) image quality did not meet measurement requirements, (3) polycystic kidney disease, (4) contraindications for MRI examination, and (5) acute renal insufficiency. Twenty healthy volunteers who had no history of vascular diseases, hypertension, or diabetes mellitus were also recruited and served as controls.

Serum creatinine (SCr) and 24-h urinary protein (24 h-UPRO) were measured in all participants 1 day before MRI examinations. The eGFR was calculated using the Chronic Kidney Disease Epidemiology Collaboration formula [20]. The CKD patients were divided into the CKD with normal eGFR group (eGFR ≥ 90 mL/min/1.73 m^2) and CKD with abnormal eGFR group (eGFR < 90 mL/min/1.73 m^2).

MRI protocols

MRI examinations were performed using a 3 Tesla MRI system (MAGNETOM Prisma, Siemens Healthcare) with an 18-channel body array coil and an integrated 32-channel spine coil as the receiver. All subjects were required to fast for at least 6 h before MRI examinations. All relevant scan parameters are summarized in Table 1. First, coronal T2 and axial T1 weighted images covering bilateral kidneys were obtained for anatomic characterization. A prototypic three-dimensional TGSE sequence with the pseudo-continuous arterial spin labeling (pCASL) scheme was applied to evaluate renal

Table 1 MRI protocol parameters

	T1WI	T2WI	ASL	IVIM-DWI
Sequence type	VIBE	HASTE	TGSE pCASL	Zoomed-DWI
Orientation	Transversal	Coronal	Coronal	Coronal
Respiratory pattern	Breath-hold	Breath-hold	Free-breathing	Free-breathing
TR/TE (ms)	3.3/1.3	1200/95	5000/19.25	4000/54
Voxel size (mm^3)	1.2 × 1.2 × 3.0	1.2 × 1.2 × 4.0	4.7 × 4.7 × 5.0	2.0 × 1.7 × 5.0
FOV (mm^2)	380 × 308	380 × 356	300 × 150	400 × 168
Matrix	320 × 240	320 × 272	64 × 32	200 × 100
Slices	60	30	16	15
Acceleration factor	4 (CAIPIRINHA)	3 (GRAPPA)	1	2 (GRAPPA)
Acquisition time	15 s	40 s	5 min	5 min 54 s

ASL, arterial spin labeling; *IVIM-DWI*, intravoxel incoherent motion diffusion-weighted imaging; *VIBE*, volumetric interpolated breath-hold examination; *HASTE*, half-Fourier-acquired single-shot turbo spin echo; *TR*, repetition time; *TE*, echo time; *FOV*, field of view; *CAIPIRINHA*, controlled aliasing in parallel imaging results in higher acceleration; *GRAPPA*, generalized autocalibrating partially acquisitions

perfusion non-invasively. To minimize the effects of respiratory movement on perfusion imaging, retrospective registration of the image volumes was performed before averaging. The T1 of blood at 3 Tesla was 1.6 s, blood-tissue water partition coefficient was 0.9 mL/100 g, inversion efficiency was 0.98, and the arrival time of labeled blood was 750 ms. Inflowing arterial blood suppression and background suppression were both performed; post labeling delay and the labeling duration were 1500 ms. Prototypic zoomed field-of-view echo-planar IVIM-DWI was performed in coronal sections with 10 b values (0, 25, 50, 80, 100, 150, 300, 500, 800, and 1000 s/mm^2). To mitigate the effects of diffusion anisotropy, diffusion was encoded in four directions and then combined to trace-weighted images. Furthermore, motion registration, slight rotation of the field-of-excitation [21], and complex averaging [22] were applied to further enhance the image quality of IVIM-DWI.

Image analysis

All images were analyzed by the first author, and regions of interest (ROIs) were confirmed by an experienced radiologist. Both of them were blinded to clinical information of the participants. The prototype software Body Diffusion Toolbox (Siemens Healthcare) was used to generate IVIM-DWI parameter maps (D, D*, and f). The D, D*, and f maps were calculated by fitting all b values to the biexponential model described by Le Bihan et al [6]. Quantitative renal blood flow (RBF) maps were generated inline after data acquisition according to the formula used by previous studies [18, 23]. When drawing the ROIs, areas with cysts, artifacts, collecting system, or vascular structures were excluded. Two coronal planes near the kidney hilum were selected for drawing ROIs. Two ROIs (70–110 voxels each) covering the entire renal cortex for each kidney were manually drawn on the IVIM-DWI parameters and RBF maps. The renal cortical D, D*, f, and RBF values of each kidney were obtained by averaging the separate readings of cortical ROIs. The MRI parameter values of bilateral kidneys were averaged for subsequent statistical analysis as eGFR reflects the overall function of both kidneys. Furthermore, we randomly selected functional MRI images of 18 subjects to assess the test-retest reliability of the IVIM-DWI parameters and RBF by using the intraclass correlation coefficients (ICC).

Statistical analysis

Statistical analysis was performed with SPSS v. 22.0, Prism 5.0 (GraphPad Software), and MedCalc software (version 15.8). The renal cortical MRI parameters of the left and right kidneys were compared using a paired samples *t*-test. Data are presented as the mean ± standard deviation (SD). One-way analysis of variance or nonparametric Kruskal-Wallis test was used to compare laboratory indexes, clinical indexes, and renal cortical MRI parameters among the control group, CKD with normal eGFR group, and CKD with abnormal eGFR group, as appropriate. The post hoc multiple pairwise comparisons were performed by using the Tukey test. Furthermore, the correlation between biochemical index (SCr, 24 h-UPRO, and eGFR) and renal cortical MRI parameters (RBF, D, D*, and f) of subjects was evaluated by Spearman correlation analysis. The receiver operating characteristic (ROC) curves were generated to assess the diagnostic performance of the MRI parameters for discriminations among the three groups. The area under the curve (AUC), sensitivity, specificity, and optimal cut-off values were calculated, and the AUCs were compared by DeLong's test [24]. A two-sided p value < 0.05 was considered statistically significant.

Table 2 Clinical and laboratory characteristics of the subjects in this study

	Control group (n = 20)	Normal eGFR group (n = 26)	Abnormal eGFR group (n = 28)	p value
Age (yr)	46.5 ± 9.4	42.5 ± 9.6	47.5 ± 9.8	0.15
Sex (male/female)	9/11	14/12	15/13	0.80
Serum creatinine (μmol/L)	56.7 ± 12.7	71.6 ± 12.9	158.3 ± 78.7	< 0.05
Proteinuria (g/24 h)	0.1 ± 0.0	1.1 ± 1.0	4.1 ± 3.9	< 0.05
eGFR (mL/min/1.73 m^2)	120.6 ± 7.6	111.5 ± 15.4	50.7 ± 21.6	< 0.05

eGFR, estimated glomerular filtration rate. One-way analysis of variance or nonparametric Kruskal-Wallis test was used to compare clinical and laboratory characteristics among the three groups, as appropriate

Results

Clinical and laboratory characteristics

The 54 CKD patients (CKD with normal eGFR group, n = 26; CKD with abnormal eGFR group, n = 28) and 20 healthy volunteers (control group) were included in this study. Four CKD patients with image artifacts and two CKD patients with renal cysts were excluded. The clinical and laboratory characteristics of the three groups are shown in Table 2. No significant differences were found in age and sex among the three groups ($p > 0.05$). Not surprisingly, CKD patients in the abnormal eGFR group had significantly higher SCr and 24 h-UPRO, and lower eGFR than those in the normal eGFR group and the control group (all $p < 0.05$). However, there were no significant differences in SCr, 24 h-UPRO, or eGFR between the CKD with normal eGFR group and control group ($p > 0.05$). Typical examples of IVIM-DWI and ASL parameter maps are shown in Fig. 1.

Comparison of MRI parameters

The intraclass correlation coefficients of the cortical D, D*, f, and RBF values were 0.86 (95% confidence interval [CI], 0.66 to 0.94), 0.95 (95% CI, 0.87 to 0.98), 0.92 (95% CI, 0.81 to 0.97), and 0.86 (95% CI, 0.67 to 0.95), respectively. No significant difference in the renal cortical MRI parameters was found between the left and right kidneys. The renal cortical D, D*, f, and RBF values showed statistically significant differences among the three groups. Figure 2 and Table 3 show that renal cortical f and RBF values in the control group were significantly higher than those in the CKD with normal eGFR group ($p < 0.05$). Furthermore, renal cortical D*, f, and RBF values decreased significantly in the CKD with abnormal eGFR group compared with the control group ($p < 0.05$) and CKD with normal eGFR group ($p < 0.05$). However, renal cortical D values did not significantly differ between the CKD with abnormal eGFR group and CKD with normal eGFR group ($p > 0.05$).

Correlations between SCr, 24 h-UPRO, eGFR, and renal cortical MRI parameters

A negative correlation was observed between renal cortical D ($r = -0.294$), D* ($r = -0.515$), f ($r = -0.715$), and RBF ($r = -0.560$) values and SCr, as well as between renal cortical D ($r = -0.320$), D* ($r = -0.462$), f ($r = -0.609$), and RBF ($r = -0.634$) values and 24 h-UPRO, while eGFR was significantly positively correlated with renal cortical MRI parameters (D: $r = 0.299$, D*: $r = 0.569$, f: $r = 0.733$, RBF: $r = 0.586$) (all $p < 0.05$) (Fig. 3 and Table 4). Noticeably, there was a positive correlation between renal cortical f and RBF values ($r = 0.613$, $p < 0.05$).

Diagnostic performance of renal cortical MRI parameters for discriminating CKD patients from the control group

As demonstrated in Table 5 and Fig. 4, renal cortical RBF, D, D*, and f values could distinguish CKD patients from the control group with an AUC ranging from 0.725 to 0.947. By

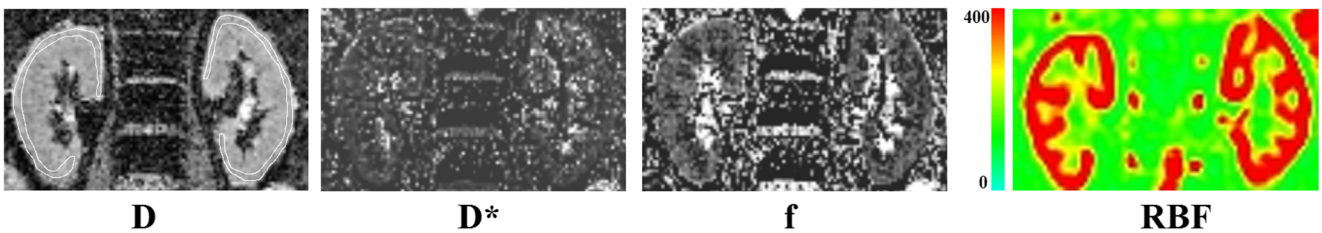

Fig. 1 Typical examples of IVIM-DWI and ASL parameter maps

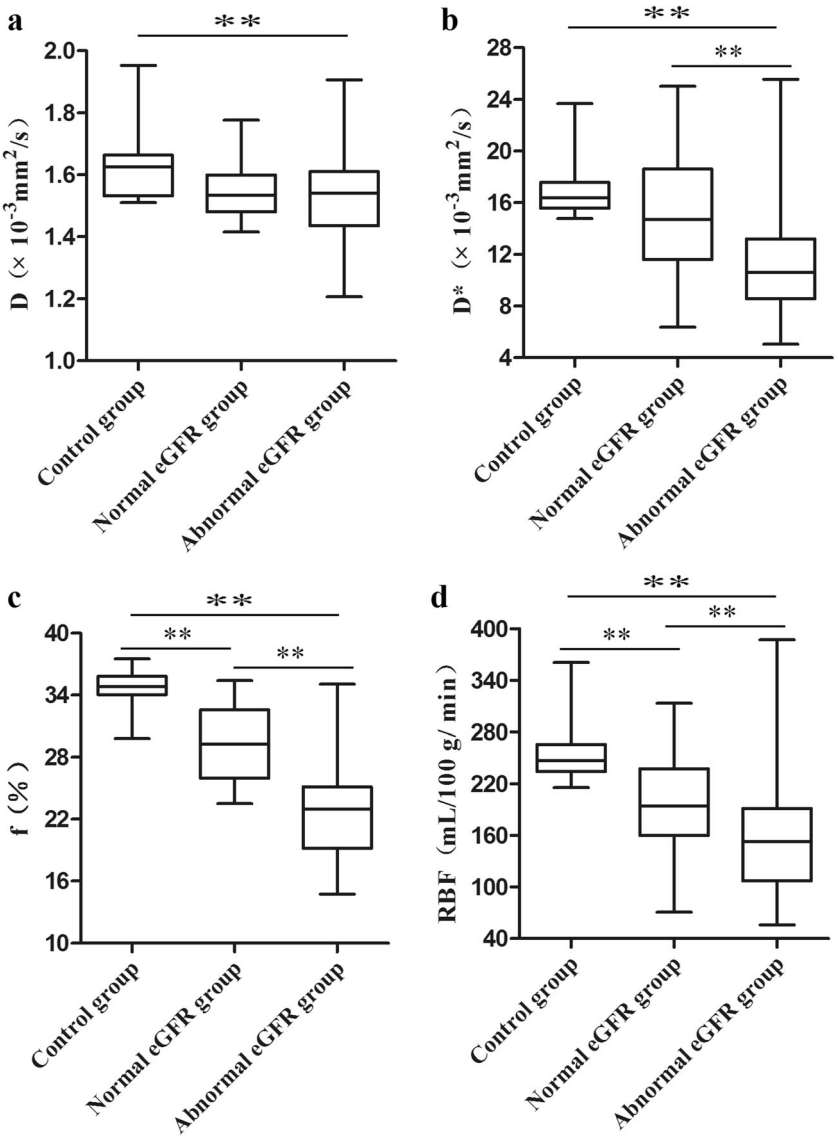

Fig. 2 Distributions of renal cortical D (**a**), D* (**b**), f (**c**), and RBF (**d**) values of control group, normal eGFR group, and abnormal eGFR group. $p < 0.05$(**)

comparison, the best-performing parameter was renal cortical f value, yielding an AUC of 0.947 (95% CI, 0.869–0.986), specificity of 85.0% (95% CI, 62.1–96.8%), and sensitivity of 94.4% (95% CI, 84.6–98.8%) under the optimal cut-off value of 33.58% (Fig. 4). Subsequent analysis revealed that the AUC of renal cortical f value was significantly larger than that

Table 3 The renal cortical MRI parameters of the subjects in this study

	Control group	Normal eGFR group	Abnormal eGFR group	*p* value	p^1 value	p^2 value	p^3 value
D ($\times 10^{-3}$ mm^2/s)	1.62 ± 0.10	1.55 ± 0.09	1.52 ± 0.15	< 0.05	0.07	< 0.05	0.80
D* ($\times 10^{-3}$ mm^2/s)	16.78 ± 2.02	14.98 ± 4.87	11.56 ± 4.40	< 0.05	0.31	< 0.05	< 0.05
f (%)	34.50 ± 2.05	29.32 ± 3.44	22.67 ± 4.58	< 0.05	< 0.05	< 0.05	< 0.05
RBF (mL/100 g/min)	253.79 ± 31.60	197.60 ± 52.45	157.44 ± 66.62	< 0.05	< 0.05	< 0.05	< 0.05

D, true diffusion coefficient; *D**, pseudo-diffusion coefficient; *f*, perfusion fraction; *RBF*, renal blood flow

[1] Post hoc paired comparisons between the control group and normal eGFR group

[2] Post hoc paired comparisons between the control group and abnormal eGFR group

[3] Post hoc paired comparisons between the normal eGFR group and abnormal eGFR group

One-way analysis of variance was used to compare renal cortical MRI parameters among the three groups. The post hoc multiple pairwise comparisons were performed by using the Tukey test

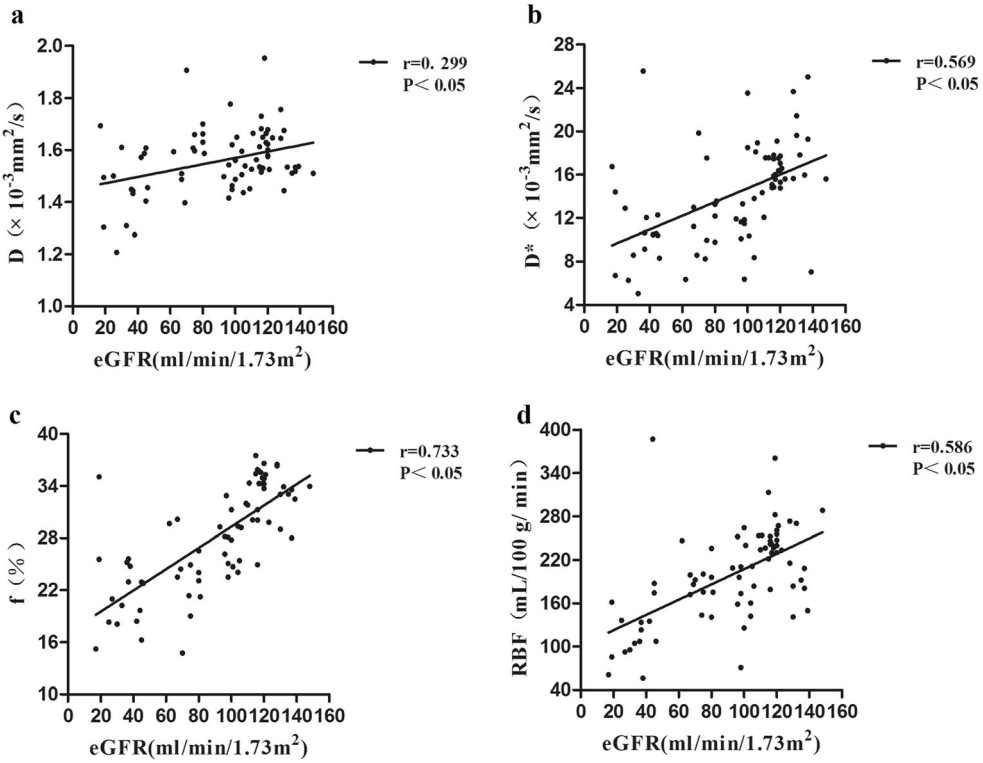

Fig. 3 Correlations between eGFR and renal cortical D (**a**), D* (**b**), f (**c**), and RBF (**d**) values

of D and D* ($p < 0.05$). Nevertheless, the AUC of renal cortical f value was not statistically different from that of cortical RBF value ($p > 0.05$).

Diagnostic performance of eGFR and renal cortical MRI parameters for differentiating the CKD with normal eGFR group from the control group

The results are shown in Table 5 and Fig. 4. Renal cortical RBF, D, D*, f values, and eGFR could identify CKD patients with normal eGFR with an AUC ranging from 0.612 to 0.917. By comparison, the best-performing parameter was renal cortical f value, yielding an AUC of 0.917 (95% CI, 0.798–0.978), specificity of 85.0% (95% CI, 62.1–96.8%), and sensitivity of 92.3% (95% CI, 74.9–99.1%) under the optimal cut-off value of 33.58% (Fig. 4). Subsequent analysis revealed that the AUC of the renal cortical f value was significantly larger than that of eGFR ($p < 0.05$). Nevertheless, no significant differences were seen in the AUCs between renal cortical RBF and f values ($p > 0.05$).

Discussion

There are growing interests in searching for auxiliary or alternative techniques to assess renal perfusion and function noninvasively [25, 26]. The main findings of this study demonstrated that IVIM-DWI and ASL allowed the noninvasive detection of early-stage kidney injury in CKD patients, even in CKD patients with normal eGFR. Furthermore, renal

Table 4 Correlations of the renal cortical MRI parameters with SCr, 24 h-UPRO, and eGFR

	SCr (μmol/L)		24 h-UPRO (g/24 h)		eGFR (mL/min/1.73 m^2)	
	r	*p*	*r*	*p*	*r*	*p*
D ($\times 10^{-3}$ mm^2/s)	−0.294	0.011	−0.320	0.005	0.299	0.010
D* ($\times 10^{-3}$ mm^2/s)	−0.515	0.000	−0.462	0.000	0.569	0.000
f (%)	−0.715	0.000	−0.609	0.000	0.733	0.000
RBF (mL/100 g/min)	−0.560	0.000	−0.634	0.000	0.586	0.000

D, true diffusion coefficient; *D**, pseudo-diffusion coefficient; *f*, perfusion fraction; *RBF*, renal blood flow; *SCr*, serum creatinine; *24 h-UPRO*, 24-h urinary protein; *eGFR*, estimated glomerular filtration rate

The correlation between biochemical index (SCr, 24 h-UPRO, and eGFR) and renal cortical MRI parameters (RBF, D, D*, and f) of subjects was evaluated by Spearman correlation analysis

Table 5 Diagnostic performance of eGFR and renal cortical MRI parameters

Comparison	Cut-off value	AUC (95% *CI*)	Sensitivity (%) (95% *CI*)	Specificity (%) (95% *CI*)	*p*
Control group (n = 20) vs CKD patients (n = 54)					0.7225[a]
D ($\times10^{-3}$ mm^2/s)	≤ 1.51	0.725 (0.609–0.822)	42.6 (29.2–56.8)	100.0 (83.2–100.0)	0.0007[b]
D* ($\times10^{-3}$ mm^2/s)	≤ 14.41	0.752 (0.638–0.845)	68.5 (54.4–80.5)	100.0 (83.2–100.0)	0.0262[c]
f (%)	≤ 33.58	0.947 (0.869–0.986)	94.4 (84.6–98.8)	85.0 (62.1–96.8)	0.0009[d]
RBF (mL/100 g/min)	≤ 211.22	0.884 (0.789–0.947)	79.6 (66.5–89.4)	100.0 (83.2–100.0)	0.0452[e]
					0.1040[f]
Control group (n = 20) vs normal eGFR group (n = 26)					
D ($\times10^{-3}$ mm^2/s)	≤ 1.56	0.735 (0.584–0.854)	73.1 (52.2–88.4)	70.0 (45.7–88.1)	0.1213[1]
D* ($\times10^{-3}$ mm^2/s)	≤ 14.34	0.612 (0.457–0.752)	50.0 (29.9–70.1)	100.0 (83.2–100.0)	0.0403[2]
f (%)	≤ 33.58	0.917 (0.798–0.978)	92.3 (74.9–99.1)	85.0 (62.1–96.8)	0.3904[3]
RBF (mL/100 g/min)	≤ 211.22	0.827 (0.687–0.922)	69.2 (48.2–85.7)	100.0 (83.2–100.0)	
eGFR (mL/min/1.73 m^2)	≤ 110.00	0.733 (0.582–0.852)	61.5 (40.6–79.8)	100.0 (83.2–100.0)	

95% CI, 95% confidence intervals; *AUC*, area under curve; *CKD*, chronic kidney disease; *D*, true diffusion coefficient; *D**, pseudo-diffusion coefficient; *f*, perfusion fraction; *RBF*, renal blood flow; *eGFR*, estimated glomerular filtration rate

[a] D vs D*; [b] D vs f; [c] D vs RBF ; [d] D* vs f; [e] D* vs RBF; [f] f vs RBF; [1] f vs RBF; [2] f vs eGFR; [3] RBF vs eGFR

cortical f value was more capable than eGFR for distinguishing the CKD with normal eGFR group from control group. This result revealed that IVIM-DWI was a potentially useful imaging tool for identifying early-stage CKD.

Detection of early-stage CKD can help delay the progression of CKD and improves outcomes. Our study found that 48.1% of the CKD patients confirmed by renal biopsy had normal eGFR (eGFR ≥ 90 ml/min/1.73 m^2). Moreover, no significant difference in SCr, 24 h-UPRO, and eGFR was found between the CKD with normal eGFR group and control group. This result suggests that the value of routine clinical biochemical markers was limited in identifying early-stage CKD. By contrast, renal cortical f and RBF values decreased significantly in the CKD with normal eGFR group compared with the control group, which suggests that IVIM-DWI and ASL might serve as additional tools to assess the function of CKD.

We found that renal cortical D, D*, f, and RBF values decreased successively among the three groups, and renal cortical D*, f, and RBF values were significantly lower in CKD patients with abnormal eGFR than those in CKD patients with normal eGFR and healthy volunteers. These results were similar to the findings of previous studies in CKD. For example, Cai et al [27] showed that the renal cortical RBF value of CKD patients was lower than that of healthy volunteers, and renal cortical RBF values positively correlated with eGFR. Lu et al [18] found that renal cortical RBF value of healthy volunteers was significantly higher than that of CKD patients. The renal cortical RBF value in CKD patients of stages 1 and 2 was significantly higher than that in CKD patients of stages 3, 4, and 5. Furthermore, Liang et al [28] have demonstrated that renal cortical D and f values had a tendency to decrease: CKD stage 4–5 < CKD stage 1–3 < healthy volunteers in a cohort of

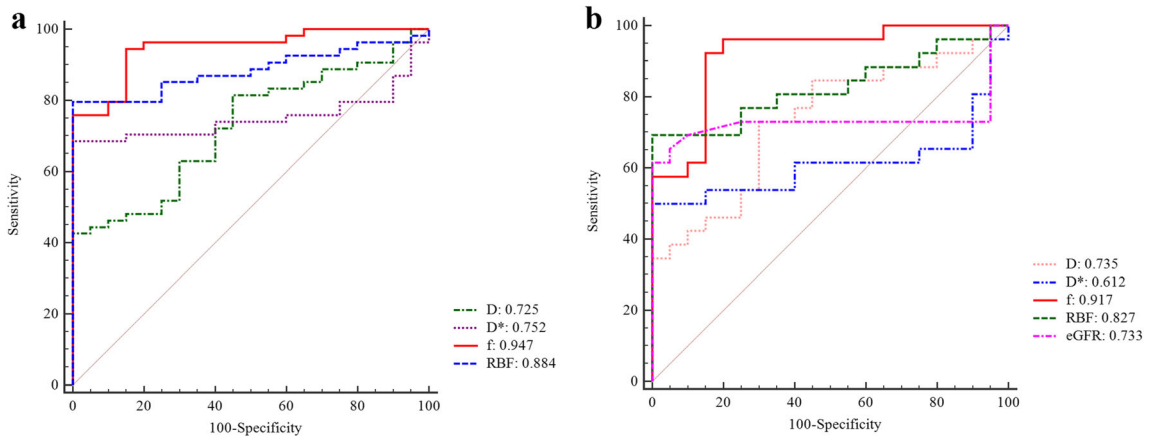

Fig. 4 Receiver operating characteristic curves for the discrimination of CKD patients from the control group (**a**) and CKD patients with normal eGFR from the control group (**b**)

74 children. So what could explain the decreased renal cortical D, D*, f, and RBF values of CKD patients in our study? We speculated that this might be explained by the following factors. Firstly, the reduced D value reflected the limitation of water molecule diffusion, which was possibly caused by the presence of fibrosis and increased cell density in the kidney parenchyma during the occurrence and development of CKD [28]. Secondly, D* and RBF values reflected the mean renal blood flow, while the f value was connected with the fraction volume of capillary blood flow, all of which could reflect blood perfusion in renal tissue [9, 18, 29]. Wang et al [16] have demonstrated that blood perfusion of renal cortex was related to peritubular capillary density, while major pathologic changes in CKD, such as tubular atrophy, glomerular sclerosis, interstitial fibrosis, and arteriolar wall thickening with degeneration, could destroy peritubular capillaries and lead to the reduction of renal cortical perfusion.

In this study, renal cortical D, D*, and f values were significantly correlated with SCr, 24 h-UPRO, and eGFR. However, in a previous study of CKD patients by Liang et al [28], only the renal parenchymal D value was significantly correlated with eGFR and SCr. The difference between our study and previous research might be caused by the following factors: firstly, the size and number of b values were different; secondly, different subjects, Liang et al recruited children, while our study included adults. Additionally, a significantly positive correlation was also found between eGFR and renal cortical RBF value, which was consistent with previous studies [18, 30, 31]. Besides, a negative correlation between SCr, 24 h-UPRO, and renal cortical RBF value was also observed. The results of our study suggest that ASL and IVIM-DWI could provide an effective tool to assess the renal injury of CKD.

ROC curve analysis supported the application of IVIM-DWI and ASL to distinguish CKD patients from healthy volunteers, as certified by its high specificity and large AUC. More importantly, our study revealed that the AUC of renal cortical f values was statistically larger than that of eGFR for the discrimination between the CKD with normal eGFR group and the control group. Therefore, we believe that IVIM-DWI may be more effective for detecting underlying pathologic injury in early-stage CKD patients with normal eGFR.

The test-retest reliability of the IVIM-DWI parameters and RBF were relatively high in our study, which was consistent with previous studies [11, 32]. Furthermore, de Boer et al [33] found poor measurement reproducibility of the RBF in renal medulla, which is likely due to the slower blood flow and lower blood perfusion in the renal medulla than that of the renal cortex. Additionally, D* and f values were related to renal blood perfusion. Hence, only the MRI parameters of the renal cortex were measured in this study.

In contrast to previous works, in this study, a free-breathing acquisition combined with motion correction strategies was applied in IVIM-DWI and ASL, which we thought was more appropriate than breath-holding and respiratory triggering technology. This was because free-breathing acquisition had a shorter scanning time than respiratory triggering technology, and it was more acceptable to patients than breath-holding technology, particularly the elderly and children [18, 31, 34].

Our study was subject to limitations that were inherent in clinical research involving human participants. Firstly, this research was performed in a single center with a relatively small number of subjects, which might affect the clinical applicability of the conclusion. Secondly, the ROI for the MRI parameters measurement was manually drawn, which might bring subjectivity bias and errors. Nonetheless, we supposed that these could be minimized, as the whole kidney was affected by diffuse nephropathy in CKD patients.

In conclusion, our study demonstrated that IVIM-DWI and ASL were potentially useful tools for identifying CKD that need renal biopsy. Moreover, IVIM-DWI and ASL showed great promise as noninvasive tools for detecting the underlying pathologic injury in early-stage CKD patients.

Funding This work was supported by the Science and Technology Guided Project of Fujian Province (grant number: 2019D025); National Natural Science Foundation of China (grant number: 82171897); Shanghai Science and Technology Committee (grant number: 19411965500); Shanghai Municipal Key Clinical Specialty (grant number: shslczdzk03202); Clinical Research Plan of SHDC (grant number: SHDC2020CR1029B); Clinical Research Project of Zhongshan Hospital, Fudan University (grant number: 2020ZSLC61); and "Science and Technology Innovation Action Plan" Star Project/Star Cultivation (Sailing Special Project) (grant number: 22YF1443700).

Declarations

Guarantor The scientific guarantor of this publication is Jianjun Zhou.

Conflict of interest Authors Caixia Fu, Bernd Kuehn, Thomas Benkert, and Robert Grimm are employees of Siemens. The remaining authors declare no relationships with any companies whose products or services may be related to the subject matter of the article.

Statistics and biometry No complex statistical methods were necessary for this paper.

Informed consent Written informed consent was obtained from all subjects in this study.

Ethical approval Institutional Review Board approval was obtained.

Methodology
- prospective
- diagnostic study/observational
- performed at one institution

References

1. Zhang L, Wang H (2009) Chronic kidney disease epidemic: cost and health care implications in China. Semin Nephrol 29(5):483–486
2. National Kidney Foundation (2002) K/DOQI clinical practice guidelines for chronic kidney disease: evaluation, classification, and stratification. Am J Kidney Dis 39(2 Suppl 1):S1–S266
3. Moledina DG, Luciano RL, Kukova L et al (2018) Kidney biopsy-related complications in hospitalized patients with acute kidney disease. Clin J Am Soc Nephrol 13(11):1633–1640
4. Kim DW, Shim WH, Yoon SK et al (2017) Measurement of arterial transit time and renal blood flow using pseudocontinuous ASL MRI with multiple post-labeling delays: feasibility, reproducibility, and variation. J Magn Reson Imaging 46(3):813–819
5. Ding Y, Zeng M, Rao S, Chen C, Fu C, Zhou J (2016) Comparison of biexponential and monoexponential model of diffusion-weighted imaging for distinguishing between common renal cell carcinoma and fat poor angiomyolipoma. Korean J Radiol 17(6):853–863
6. Le Bihan D, Breton E, Lallemand D, Aubin ML, Vignaud J, Laval-Jeantet M (1988) Separation of diffusion and perfusion in intravoxel incoherent motion MR imaging. Radiology 168(2):497–505
7. van Baalen S, Leemans A, Dik P, Lilien MR, Ten HB, Froeling M (2017) Intravoxel incoherent motion modeling in the kidneys: comparison of mono-, bi-, and triexponential fit. J Magn Reson Imaging 46(1):228–239
8. Caroli A, Schneider M, Friedli I et al (2018) Diffusion-weighted magnetic resonance imaging to assess diffuse renal pathology: a systematic review and statement paper. Nephrol Dial Transpl 33(suppl_2):i29–i40
9. Le Bihan D (2019) What can we see with IVIM MRI? Neuroimage 187:56–67
10. Li Q, Li J, Zhang L, Chen Y, Zhang M, Yan F (2014) Diffusion-weighted imaging in assessing renal pathology of chronic kidney disease: a preliminary clinical study. Eur J Radiol 83(5):756–762
11. Mao W, Zhou J, Zeng M et al (2018) Chronic kidney disease: pathological and functional evaluation with intravoxel incoherent motion diffusion-weighted imaging. J Magn Reson Imaging 47(5):1251–1259
12. Woo S, Cho JY, Kim SY, Kim SH (2018) Intravoxel incoherent motion MRI-derived parameters and T2* relaxation time for non-invasive assessment of renal fibrosis: an experimental study in a rabbit model of unilateral ureter obstruction. Magn Reson Imaging 51:104–112
13. Mao W, Zhou J, Zeng M et al (2018) Intravoxel incoherent motion diffusion-weighted imaging for the assessment of renal fibrosis of chronic kidney disease: a preliminary study. Magn Reson Imaging 47:118–124
14. Ebrahimi B, Rihal N, Woollard JR, Krier JD, Eirin A, Lerman LO (2014) Assessment of renal artery stenosis using intravoxel incoherent motion diffusion-weighted magnetic resonance imaging analysis. Invest Radiol 49(10):640–646
15. Xie Y, Li Y, Wen J et al (2018) Functional evaluation of transplanted kidneys with reduced field-of-view diffusion-weighted imaging at 3T. Korean J Radiol 19(2):201–208
16. Wang W, Yu Y, Wen J et al (2019) Combination of functional magnetic resonance imaging and histopathologic analysis to evaluate interstitial fibrosis in kidney allografts. Clin J Am Soc Nephrol 14(9):1372–1380
17. Ritt M, Janka R, Schneider MP et al (2010) Measurement of kidney perfusion by magnetic resonance imaging: comparison of MRI with arterial spin labeling to para-aminohippuric acid plasma clearance in male subjects with metabolic syndrome. Nephrol Dial Transplant 25(4):1126–1133
18. Lu F, Yang J, Yang S et al (2021) Use of three-dimensional arterial spin labeling to evaluate renal perfusion in patients with chronic kidney disease. J Magn Reson Imaging 54(4):1152–1163
19. Hueper K, Gutberlet M, Rong S et al (2014) Acute kidney injury: arterial spin labeling to monitor renal perfusion impairment in mice-comparison with histopathologic results and renal function. Radiology 270(1):117–124
20. Levey AS, Stevens LA, Schmid CH et al (2009) A new equation to estimate glomerular filtration rate. Ann Intern Med 150(9):604–612
21. Finsterbusch J (2012) Improving the performance of diffusion-weighted inner field-of-view echo-planar imaging based on 2D-selective radiofrequency excitations by tilting the excitation plane. J Magn Reson Imaging 35(4):984–992
22. Kordbacheh H, Seethamraju RT, Weiland E et al (2019) Image quality and diagnostic accuracy of complex-averaged high b value images in diffusion-weighted MRI of prostate cancer. Abdom Radiol (NY) 44(6):2244–2253
23. Robson PM, Madhuranthakam AJ, Dai W, Pedrosa I, Rofsky NM, Alsop DC (2009) Strategies for reducing respiratory motion artifacts in renal perfusion imaging with arterial spin labeling. Magn Reson Med 61(6):1374–1387
24. DeLong ER, DeLong DM, Clarke-Pearson DL (1988) Comparing the areas under two or more correlated receiver operating characteristic curves: a nonparametric approach. Biometrics 44(3):837–845
25. Zhang JL, Lee VS (2020) Renal perfusion imaging by MRI. J Magn Reson Imaging 52(2):369–379
26. Zhou JY, Wang YC, Zeng CH, Ju SH (2018) Renal functional MRI and its application. J Magn Reson Imaging 48(4):863–881
27. Cai YZ, Li ZC, Zuo PL et al (2017) Diagnostic value of renal perfusion in patients with chronic kidney disease using 3D arterial spin labeling. J Magn Reson Imaging 46(2):589–594
28. Liang P, Chen Y, Li S et al (2021) Noninvasive assessment of kidney dysfunction in children by using blood oxygenation level-dependent MRI and intravoxel incoherent motion diffusion-weighted imaging. Insights Imaging 12(1):146
29. Cheng ZY, Feng YZ, Hu JJ et al (2020) Intravoxel incoherent motion imaging of the kidney: the application in patients with hyperuricemia. J Magn Reson Imaging 51(3):833–840
30. Mora-Gutierrez JM, Garcia-Fernandez N, Slon RM et al (2017) Arterial spin labeling MRI is able to detect early hemodynamic changes in diabetic nephropathy. J Magn Reson Imaging 46(6):1810–1817
31. Li LP, Tan H, Thacker JM et al (2017) Evaluation of renal blood flow in chronic kidney disease using arterial spin labeling perfusion magnetic resonance imaging. Kidney Int Rep 2(1):36–43
32. Gillis KA, McComb C, Foster JE et al (2014) Inter-study reproducibility of arterial spin labelling magnetic resonance imaging for measurement of renal perfusion in healthy volunteers at 3 Tesla. BMC Nephrol 15:23
33. de Boer A, Harteveld AA, Stemkens B et al (2021) Multiparametric renal MRI: an intrasubject test-retest repeatability study. J Magn Reson Imaging 53(3):859–873
34. Nery F, Buchanan CE, Harteveld AA et al (2020) Consensus-based technical recommendations for clinical translation of renal ASL MRI. MAGMA 33(1):141–161